Laser-Driven Ultrafast Field Propagation on Solid Surfaces

K. Quinn,[1,*] P. A. Wilson,[1] C. A. Cecchetti,[1,†] B. Ramakrishna,[1] L. Romagnani,[1] G. Sarri,[1] L. Lancia,[2] J. Fuchs,[2] A. Pipahl,[3] T. Toncian,[3] O. Willi,[3] R. J. Clarke,[4] D. Neely,[4] M. Notley,[4] P. Gallegos,[4,5] D. C. Carroll,[5] M. N. Quinn,[5] X. H. Yuan,[5] P. McKenna,[5] T. V. Liseykina,[6,‡] A. Macchi,[7] and M. Borghesi[1]

[1]*Department of Physics and Astronomy, Queen's University Belfast, Belfast BT7 1NN, United Kingdom*
[2]*Laboratoire pour l'Utilisation des Lasers Intenses, École Polytechnique, 91128 Palaiseau, France*
[3]*Institut für Laser–und Plasmaphysik, Heinrich-Heine-Universität, D-40225 Düsseldorf, Germany*
[4]*Central Laser Facility, Rutherford Appleton Laboratory, Chilton, Oxfordshire OX11 0QX, United Kingdom*
[5]*SUPA, Department of Physics, University of Strathclyde, Glasgow G4 0NG, United Kingdom*
[6]*Max Planck Institute for Nuclear Physics, Heidelberg, Germany*
[7]*CNR/INFM/polyLAB, Dipartimento di Fisica "E. Fermi," Pisa, Italy*

(Received 28 January 2009; published 14 May 2009)

The interaction of a 3×10^{19} W/cm^2 laser pulse with a metallic wire has been investigated using proton radiography. The pulse is observed to drive the propagation of a highly transient field along the wire at the speed of light. Within a temporal window of 20 ps, the current driven by this field rises to its peak magnitude $\sim 10^4$ A before decaying to below measurable levels. Supported by particle-in-cell simulation results and simple theoretical reasoning, the transient field measured is interpreted as a charge-neutralizing disturbance propagated away from the interaction region as a result of the permanent loss of a small fraction of the laser-accelerated hot electron population to vacuum.

DOI: 10.1103/PhysRevLett.102.194801 PACS numbers: 41.75.Jv, 52.38.Kd, 52.57.Kk

The processes by which the relativistic electrons generated in intense ($I > 10^{18}$ W/cm^2) laser-solid interactions transfer their energy from the focal spot to the bulk target remain elusive, yet further investigation into such transport mechanisms is vital, not least of all, to the realization of fast ignition [1]. The incidence of a high-intensity pulse onto a cone-wire target has been used to study the mechanisms by which ignition energy might be delivered to the core [2]. The production of hot electron currents in solid targets is also the basis for the growing field of laser-driven ion acceleration [3]. It has been shown that the adaptation of the divergent, broadband proton beams generated via target normal sheath acceleration (TNSA) [3] to a range of applications [3,4] might be facilitated by the development of one of two schemes for the optimization of a laser-driven proton beam to its minimal bandwidth and divergence angle [5,6], both of which are related to the laser-induced ultrafast (picosecond-time scale) charging of a solid. The development of fast rise-time laser-driven Z pinches, meanwhile, also demands a thorough knowledge of the transient currents induced in laser-wire interactions [7].

While the global charging of a solid irradiated at high intensity has been reported previously [8,9], the propagation mechanism of the related charging fields remains unclear, and local current flows have not yet been directly observed.

In this Letter, we present the experimental observation of the highly transient laser-driven current induced in the interaction of an intense (3×10^{19} W/cm^2) pulse with a metallic wire target. The velocity at which the charge pulse moves along the wire is confidently measured by a novel experimental arrangement to be $\sim c$. The measurements are consistent with a current which rises to a peak magnitude of 8 kA before decaying to below measurable levels over 20 ps. All measurements were performed by employing a TNSA proton beam as a charged particle probe of the electromagnetic fields set up by the interaction pulse in the region of the target. Some 3×10^{11} electrons are calculated to have been drawn toward the interaction region past the cross section of measurement, a figure consistent with a simple model of the target charging.

The proton radiography or imaging technique [10] operates on the principle that the Lorentz deflections impinged upon the constituent protons of the probe beam act as a measure of the E and B fields set up in the interaction region. Dosimetric radiochromic film (RCF) [11] is commonly employed transverse to the incident beam as a proton detector, providing spatially and energetically resolved detection of the incident proton beam when used in a layered configuration. Each RCF layer may then be related to a proton energy E_p by calculating the distance into the film pack at which the Bragg peak occurs as a function of E_p. The probing time assigned to a given layer is then given by $t_{\text{probe}} = d(m_p/2E_p)^{1/2}$, where d is the distance from the proton source to the point of interest at the target and m_p is the proton mass. The evolution of the electric and magnetic fields set up as a result of the interaction pulse may hence be inferred with μm ps spatiotemporal resolution by comparing the experimental proton density behavior at the detector with the results of three-dimensional (3D) particle-tracing simulations [10].

The experiment was conducted on the VULCAN Petawatt laser system [12]. One-tenth of the cross section

of the main 260 J, picosecond-duration, 60 cm beam entering the target chamber was diverted *in situ* via a 235 mm-diameter pickup mirror to provide the interaction pulse CPA_2 [13], which was focused down to an $8 \times 4\ \mu m^2$ spot to give an on-target intensity of $3 \times 10^{19}\ W/cm^2$. The remainder of the main beam (CPA_1) was focused down to an area of $5 \times 4\ \mu m^2$ by a 1 m off-axis parabola onto a 20 μm Au foil to accelerate the proton beam for probing of the interaction. A 50 ps optical delay was applied to CPA_2 so that the target was completely enveloped in the probe beam at the time of the interaction. The cutoff energy of the proton beam accelerated by the $4 \times 10^{20}\ W/cm^2$ CPA_1 pulse was roughly 25 MeV so that, when combined with the RCF stack, observation of the wire was provided over 40 ps.

We first studied the interaction of CPA_2 with a 125 μm-diameter gold wire in a vertical orientation [shot *A*; see Fig. 1(a)]. Measurements were performed at the *zero level* of the probe beam (the level at which protons emitted from the source have no vertical component of velocity). As shown in Fig. 2, over a temporal window of some 20 ps, the extent of the deflections imposed upon the probe protons as they pass the wire increases to its maximum before decaying. This feature is interpreted as being caused by the transient charging and subsequent discharging of the wire as a result of the CPA_2 interaction. That this electrical charging is positive is revealed by the fact that proton density "pileups" are visible on either side of the wire image while the central region is depleted (protons have been deflected *away* from the wire).

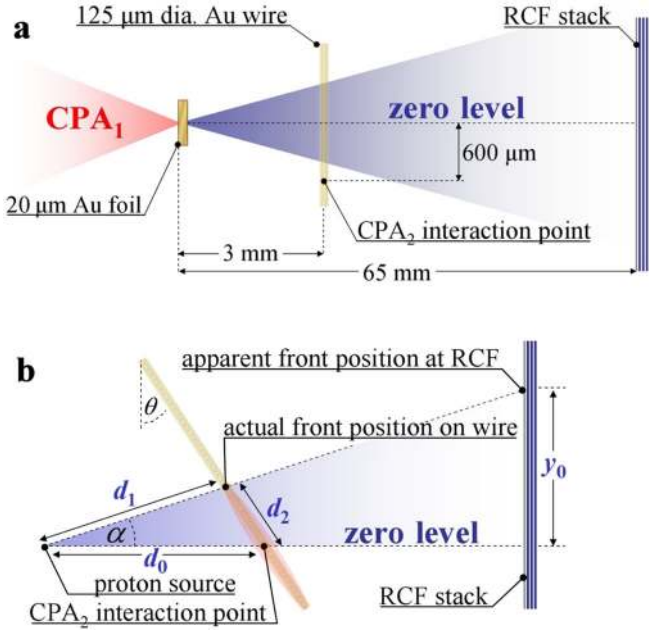

FIG. 1 (color online). (a) Schematic describing the experimental setup used on shot *A*. (b) The corresponding setup used on shot *B*. In both cases, CPA_2 strikes into the page.

The fields set up as a result of the laser-wire interaction were modeled in the particle tracer. If E_s is the strength of the outwards-pointing radial electric field at the wire surface and r_w the wire radius, then by assuming that (i) positive charge is contained exclusively within the wire and (ii) the negative charge density outside the wire is low compared to the positive charge density inside, the electric field strength at a given radial distance r from the axis may be approximated by $E_s(r_w/r)$ for $r \geq r_w$. The electric field is largely absent for $r < r_w$, meanwhile, falling to $1/e$ of its maximum strength within a skin depth of the wire surface. The azimuthal magnetic field associated with current propagation along the wire is in turn computed via application of Ampère's law, although particle-tracing simulations demonstrated that deflections to the probe protons could be attributed exclusively to the E field as long as the maximum B-field strength did not exceed 100 T.

For each RCF layer, the value of E_s was repeatedly varied in the particle tracer until a match was obtained between the simulated proton density behavior at the detector and that recorded experimentally. The maximum value of E_s was hence determined to be $8 \times 10^9\ V/m$. Because of the fact that the wire is oriented vertically, d does not vary significantly within the field of view of the probe beam, and each RCF layer in the data set for shot *A* corresponds effectively to a *discrete* probing time. Hence, although there is some indication in Fig. 2 that a charging front might be propagating along the wire, such a front is not clearly resolved.

Relativity dictates that, for the whole target to have become positively charged, such a front must have traversed the wire at some finite velocity $v_f \leq c$. On shot *B*, a small but crucial change was made to the experimental setup to enable the resolution of such a charging front [see Fig. 1(b)]. The experiment was repeated under identical

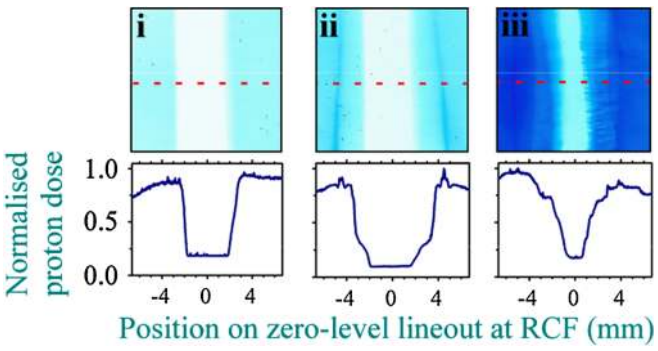

FIG. 2 (color online). Samples of RCF data from shot *A* describing the CPA_2 interaction on a vertical 125 μm Au wire. The dashed red line marks the zero level of the probe proton beam. Corresponding proton density lineouts taken across the zero level are shown below each RCF image. Relative to the time of arrival of the CPA_2 interaction pulse, the probing times depicted by each layer are (i) 0, (ii) 10, and (iii) 25 ps.

conditions in terms of CPA_2 intensity and pulse duration and wire material and diameter. The wire itself, however, was modified so as to lie an angle $\theta = 30 \pm 0.5°$ to the vertical. As a result, the protons forming the bulk of the signal on a given RCF layer, all traveling at the same velocity, will have probed different points along the wire at different times based on their initial elevation angle relative to the zero level α. In this way, *continuous* observation of the target is provided.

As shown in Fig. 3, the motion of such an electric field front up the wire is easily resolved on shot *B*. It moves away from the CPA_2 interaction point at $v_f = (0.95 \pm 0.05)c$. The data presented here, hence, represent the first experimental measurement of the velocity at which field spreads over a target in an intense laser-solid interaction. With its single-shot, multiframe capabilities, proton radiography is arguably the only diagnostic currently available with which this measurement could have been made.

The observation of the propagation of this field front away from the CPA_2 interaction point at $\sim c$ enables the result of shot *A*, in describing the evolution of the magnitude of the radial electric field at the wire surface $E_s(t)$, to be interpreted as being caused by the flow of a transient current past the zero level, the magnitude of which may be shown by application of Gauss's law and the continuity

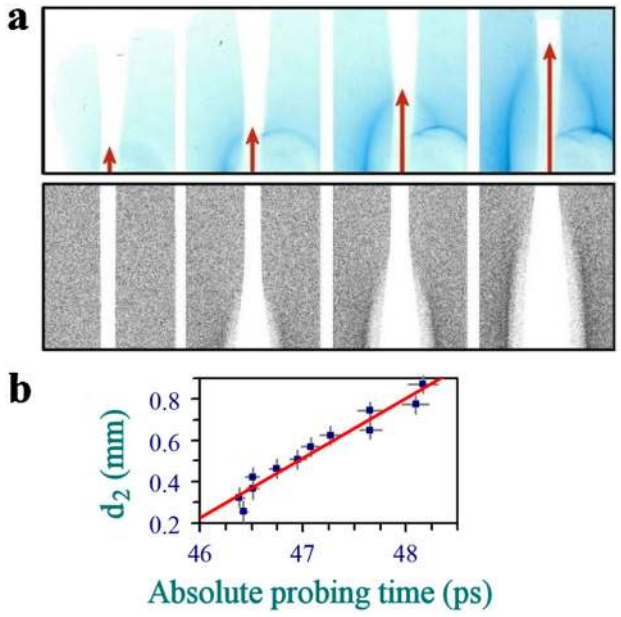

FIG. 3 (color online). (a) Selection of experimental (top) and simulated (bottom) RCF data detailing the propagation of the charging front away from interaction point on shot *B*. The front position is indicated by the red arrows. The CPA_2 interaction plasma is visible to the bottom right of each experimental image as a circular area of proton depletion. (b) Measurement of distance from interaction point (d_2) as a function of absolute probing time (relative to the acceleration of the proton beam at the source). The velocity at which the charging front moves along the wire is measured to be $(0.95 \pm 0.05)c$.

equation to be given by $I(t) = 2\pi\epsilon_0 r_w v_f E_s(t)$. This current, then, is calculated to rise to its peak value of 8.1 kA before falling to below measurable levels ($\sim$1 kA) over a temporal window of some 20 ps. At later times, $I(t)$ will relax further as laser-driven hot electrons recombine with the wire plasma; ultimately, though, global neutralization of the target is facilitated by the flow of negative charge from the effectively infinite electron reservoir of the target mount [6].

Integration of $I(t)$ over time reveals the net total number of electrons moving downwards past the zero level to be $N_0 \simeq 3 \times 10^{11}$. This contrasts starkly with the total number of hot electrons predicted to have been accelerated by CPA_2 at the beam focus. The total number of hot electrons accelerated can be estimated by the energy balance relation $N_{\text{total}} = fE(k_B T_h)^{-1}$ [14], where f is the fraction of laser energy absorbed by hot electrons, E the pulse energy, and $k_B T_h$ the hot electron temperature which is predicted by $I\lambda^2$ scaling to be 1.4 MeV [15]. By assuming 20% absorption of laser energy into hot electrons, then [16], the 30 J CPA_2 pulse is estimated to accelerate some 3×10^{13} hot electrons at its focus. A large positive electrostatic potential, however, will develop in the region of the interaction as the laser-accelerated hot electron population streams to vacuum. Only the most energetic electrons will escape the developing potential well of the target, with the remainder returning to the wire under space-charge separation.

An estimation of the number of electrons escaping to vacuum may be made by developing a simple model of the electrostatic forces at work in this system. If a Maxwellian electron population is released from an initially neutral sphere of radius r_0, the sphere will develop a progressively larger electrostatic potential as more electrons stream to vacuum. By equating the minimum electron energy required for permanent escape to the depth of the electrostatic potential energy well at the sphere surface, the fraction ξ_∞ of the N_{total} laser-accelerated electrons lost to vacuum may be estimated by

$$\frac{\ln \xi_\infty}{\xi_\infty} = -\frac{r_c}{r_0}\frac{m_e c^2}{k_B T_h} N_{\text{total}},$$

where $r_c = 2.82 \times 10^{-15}$ m is the classical electron radius [17,18]. The main source of error in the calculation of ξ_∞ comes from the choice for r_0. With this in mind, by setting the value of r_0 to the average of its maximum and minimum possible values (the 62.5 μm wire radius and 5 μm CPA_2 spot radius, respectively), the total number of electrons escaping to vacuum is estimated to be $\sim 10^{11}$. In agreement with measurements performed under similar experimental conditions [19], the model predicts that $\sim$1% of the hot electrons accelerated at the CPA_2 focus are subsequently lost to vacuum. At 3×10^{11}, then, the total number of electrons measured to have flowed past the zero level toward the interaction point is consistent with

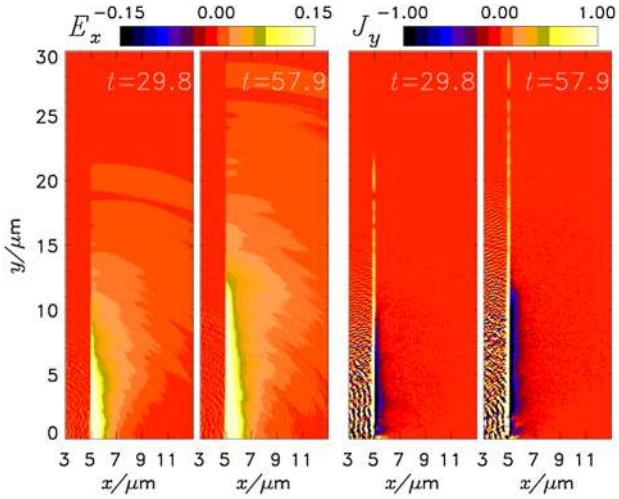

FIG. 4 (color online). PIC simulation results detailing E_x and J_y contours near the target rear surface for two different times (in femtoseconds) relative to the arrival of the pulse peak at the target front surface. The rear surface is located at $x = 5$. E_x is in units of 3.05×10^8 V/cm and J_y in units of 4.8×10^{13} A/cm^2.

the degree of global charge neutralization required following the permanent escape of a small fraction of the laser-accelerated hot electron population to vacuum.

The simulation of a scaled-down model experiment can prove fruitful in investigating the ultrafast electromagnetic dynamics of such a system. A 2D-Cartesian particle-in-cell (PIC) code [20] was hence used to simulate the interaction of a laser pulse of $\lambda = 1$ μm wavelength, 1.2×10^{19} W/cm^2 peak intensity, 100 fs duration, and 4 μm spot diameter normally incident with a plane plasma slab of electron density 10^{22} cm^{-3}. The target plasma extends over $0 < x < 5$ μm, while the pulse strikes from the left-hand side at $x = 0$, $y = 0$.

Figure 4 shows the contour levels of E_x and J_y (the components of the electric field and current density perpendicular and parallel to the target surface, respectively) at the rear side of the target. Only the $y > 0$ region is shown since E_x (J_y) is symmetrical (antisymmetrical) about $y = 0$. A propagation of both E_x and J_y along the target surface, i.e., along y, is observed. Two fronts are visible: an inner front propagating at $0.4c$ over the time interval investigated and an outer one propagating at $\simeq c$. The inner front encompasses a region of strong charge separation and current recirculation, features interpreted as being caused by the refluxing of hot electrons in and around the target. In the outer region, however, J_y is positive and is localized to a thin target surface layer. A similar feature is observed on the front side, i.e., near $x = 0$ (not shown). In our interpretation, this current, corresponding to the flow of negative charge toward the interaction region, is driven by the antennalike electromagnetic disturbance generated by transient charge separation in the region of the interaction. The disturbance propagates freely in vacuum but penetrates only the skin layer of the target. Its observed propagation velocity ($\simeq c$) and the related vacuum features of E_y and B_z (omitted for brevity) are wholly consistent with this description.

In summary, our measurements quantitatively support previously made postulations that the positive charging of solid targets irradiated at relativistic laser intensities might be attributed to hot electron escape [6–8]. Furthermore, the spread of charge in intense laser-solid interactions, a significant phenomenon for many applications in this intensity regime [1,5–7], has now been resolved directly. Importantly, supported by the results of PIC simulations, a mechanism by which such ultrafast target charging might occur has been identified.

This research was supported by: EPSRC Grants No. EP/E048668/1, No. EP/E035728/1, and No. EP/C003586/1; DFG No. TR18 and No. GK1203; the British Council Alliance Program; QUB Internationalization Funds; a DEL/AWE plc CAST grant; the STFC Direct Access Scheme; and finally, by an EPSRC/Andor Technology Dorothy Hodgkin Postgraduate grant. The support of the staff of the Central Laser Facility at RAL is gratefully acknowledged. The PIC simulations were performed at CINECA (Italy) and were sponsored by the CNR/INFM supercomputing initiative.

*kquinn09@qub.ac.uk
†Present address: Intense Laser Irradiation Laboratory, IPCF, CNR, Pisa, Italy.
‡On leave from the Institute of Computational Technologies, SD-RAS, Novosibirsk, Russia.

[1] M. Tabak *et al.*, Phys. Plasmas **1**, 1626 (1994).
[2] J. S. Green *et al.*, Nature Phys. **3**, 853 (2007).
[3] M. Borghesi *et al.*, Fusion Sci. Technol. **49**, 412 (2006), and references therein.
[4] V. Malka *et al.*, Nature Phys. **4**, 447 (2008).
[5] T. Toncian *et al.*, Science **312**, 410 (2006).
[6] S. Kar *et al.*, Phys. Rev. Lett. **100**, 105004 (2008).
[7] F. N. Beg *et al.*, Phys. Rev. Lett. **92**, 095001 (2004).
[8] M. Borghesi *et al.*, Appl. Phys. Lett. **82**, 1529 (2003).
[9] P. McKenna *et al.*, Phys. Rev. Lett. **98**, 145001 (2007).
[10] L. Romagnani *et al.*, Laser Part. Beams **26**, 241 (2008).
[11] http://www.gafchromic.com.
[12] C. N. Danson *et al.*, Nucl. Fusion **44**, S239 (2004).
[13] D. Strickland and G. Mourou, Opt. Commun. **56**, 219 (1985).
[14] A. Hauer and R. J. Mason, Phys. Rev. Lett. **51**, 459 (1983).
[15] S. Wilks and W. Kruer, IEEE J. Quantum Electron. **33**, 1954 (1997).
[16] K. B. Wharton *et al.*, Phys. Rev. Lett. **81**, 822 (1998).
[17] E. E. Fill, Phys. Plasmas **12**, 052704 (2005).
[18] V. T. Tikhonchuk, Phys. Plasmas **9**, 1416 (2002).
[19] G. Malka and J. L. Miquel, Phys. Rev. Lett. **77**, 75 (1996).
[20] G. I. Dudnikova *et al.*, Comp. Technol. **10**, 37 (2005).